ORIGINAL ARTICLE

Data-Driven Material Modeling with Functional Advection for 3D Printing of Materially Heterogeneous Objects

Christoph Bader,[1] Dominik Kolb,[1] James C. Weaver,[2] and Neri Oxman[1]

Abstract

We present a data-driven approach for the creation of high-resolution, geometrically complex, and materially heterogeneous 3D printed objects at product scale. Titled Data-driven Material Modeling (DdMM), this approach utilizes external and user-generated data sets for the evaluation of heterogeneous material distributions during slice generation, thereby enabling the production of voxel-matrices describing material distributions for bitmap-printing at the 3D printer's native voxel resolution. A bitmap-slicing framework designed to inform material property distribution in concert with slice generation is demonstrated. In contrast to existing approaches, this framework emphasizes the ability to integrate multiple geometry-based data sources to achieve high levels of control for applications in a wide variety of design scenarios. As a proof of concept, we present a case study for DdMM using functional advection, and we demonstrate how multiple data sources used by the slicing framework are implemented to control material property distributions.

Introduction

RECENT ADVANCES IN high-resolution 3D printing have enabled the design and digital fabrication of objects with unprecedented levels of structural complexity.[1,2] However, although most commonly implemented methods for the production of 3D-printable file formats rely on the generation of highly detailed surface meshes and object assemblies, they often neglect to address, or overlook, the functional need and design potential of heterogeneous material distributions that are volumetric in nature and that take full advantage of the native resolution of a 3D printer.

Modern multi-material 3D printers[3] employ photopolymerization of UV curable resins to construct 3D objects through an inkjet-like printing process by sequentially depositing layers as thin as $32 \mu m$. This high-resolution 3D printing approach enables precise spatial control over the deposition of individual material droplets, where material composition is controlled at the droplet level by defining—for each deposited material—a binary 3D voxel-matrix at the native resolution of the printer. This voxel-matrix, in turn, defines the material identity of the individual droplets and their spatial placement in space, resulting in volumetric binary material representations that can be used to define heterogeneous and continuously varying material composites at the resolution of the printer. This approach is often described as bitmap-based printing or voxel printing.[4]

Design approaches that rely solely on voxel-based representations[5,6] for 3D multi-material compositions are often challenging to scale for the production of high-resolution, large-volume models. Since commercial multi-material 3D printers can offer build envelopes as large as $40,000 \, cm^3$, defining binary 3D matrices at the native resolution of the printer results in billions of individually addressable voxels, whose representations can become overbearing in size and challenging to handle.

In the next section, we present a data-driven design approach for the production of a materially heterogeneous object, printed on a multi-material 3D printer. We showcase a Data-driven Material Modeling (DdMM) approach in the form of a case study named *Lazarus*. In contrast to previous design approaches, this approach allows us to specify multiple generated data sets, which are used to inform material distributions during slice generation. Furthermore, by partially reallocating data-transfer and data-modification to occur at the time of individual slice generation, we show how bitmap-printing in combination with function-driven material advection can be used for the design of highly complex

---

[1]Mediated Matter Group, Media Lab, Massachusetts Institute of Technology, Cambridge, Massachusetts.
[2]Wyss Institute for Biologically Inspired Engineering, Harvard University, Cambridge, Massachusetts.

Opposite page: A 3D printed model of a volumetric data-set modified with on-slice time advection. The model was printed on an Objet 500 Connex3 printer implementing Data-driven Material Modeling protocols presented in this paper. *Photo Credit:* Mediated Matter.

and intricate material distributions. Additionally, by employing a custom system for the direct input of bitmal-slices to control a 3D printer, this workflow, thus, allows us to fully leverage the native resolution of the 3D printer, highlighting the versatility, scalability, and usability of high-resolution bitmap-printing for design and engineering applications.

Data-Driven Material Modeling

Computational framework

To facilitate the use of external data sources for the design of internal material distributions, and building on previous methods,[7–9] our approach accounts for arbitrary external geometric data sets such as point-clouds, scalar and vector fields, curves and polygons, and tetrahedral meshes, with their associated attributes, as shown in the case study given next. Using these external data sources, it is possible to drive the computation of hybrid evaluated and unevaluated heterogeneous material modeling methods,[10] including distance-based,[11] source-based,[12] or synthesis-based[13] approaches during slice generation for 3D-bitmap-printing. As such, this approach is designed to handle data sources and to generate material distributions during slice generation (on-slice-time) and, therefore, it permits the incorporation of external data as the primary design element in the creative process for multi-material 3D-printed objects. Despite these significant advantages, it should be noted, however, that only computational modifications to provided data-sets can be used with this approach for which either sufficient data can be precomputed and provided during slicing, or that allow neighborhood-limited evaluation of material distributions. An overview of this workflow is provided in Figure 1.

Our framework uses polygonal meshes, with user-defined material domains as source files. Each mesh is then sliced in the print direction, resulting in a set of rasterized layers where each pixel/voxel can store, for example, material information, vectors for velocity fields, matrices, or other data structures. The resulting rasterized content is then dithered into n binary bitmaps, providing instructions for the material deposition of n materials as defined by the printer. Furthermore, as mentioned earlier, we can integrate geometry-based external or user-generated data sources of arbitrary dimensionality, which can then be used to influence the generation of the 3D-printable description at any stage of the description generation process. Figure 1(a) shows the object-representation and data-generation stages, where each object is indexed to a material-computation domain; and additional data sources can be computed and assigned for later use—for example—as part of the on-slice-time material generation step. We note that, although material-computation domains are discrete, their internal material distributions can be continuous and heterogeneous. Figure 1(b–e) illustrates the rasterization of a bitmap slice obtained from a polygonal object, where we treat the generation of a polygonal slice as an optional stage. Figure 1(c) shows a priority-ordering[8] step, describing, in a fully user-controlled manner, which material domain has higher precedence. This approach is required in cases where two or more geometric material domains are overlapping, and, as a result, a defined priority has to dictate which material will be deposited. An example of data-driven priority-ordering is shown in Figure 2.

Figure 1(e) illustrates the on-slice-time data-transfer and data-modification step, whereby user-generated and external data sources, such as scalar and vector fields, from, for
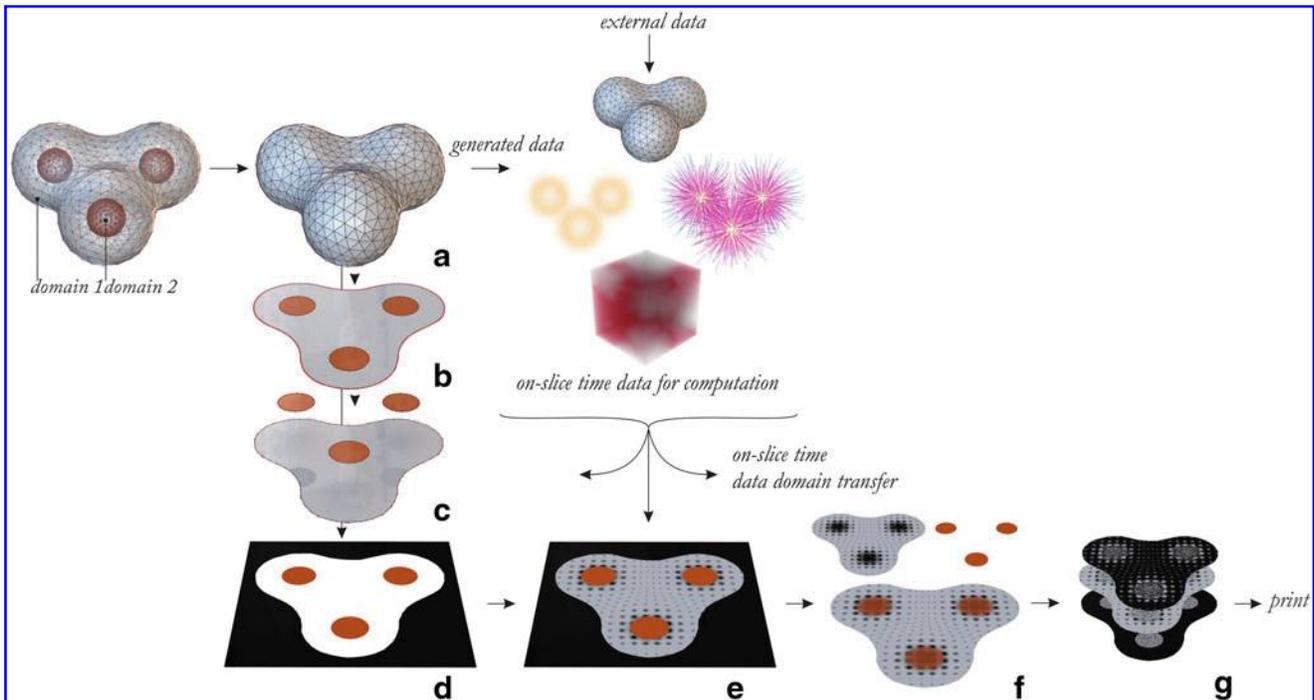

FIG. 1. A data-driven computational framework for the production of bitmap-printable parts: (a) Object representation and data generation; (b) optional generation of a polygonal slice; (c) priority-ordering of specified material domains; (d) rasterization; (e) on-slice-time data-transfer and data-modification; (f) composition; (g) material dithering and direct bitmap-printing system.
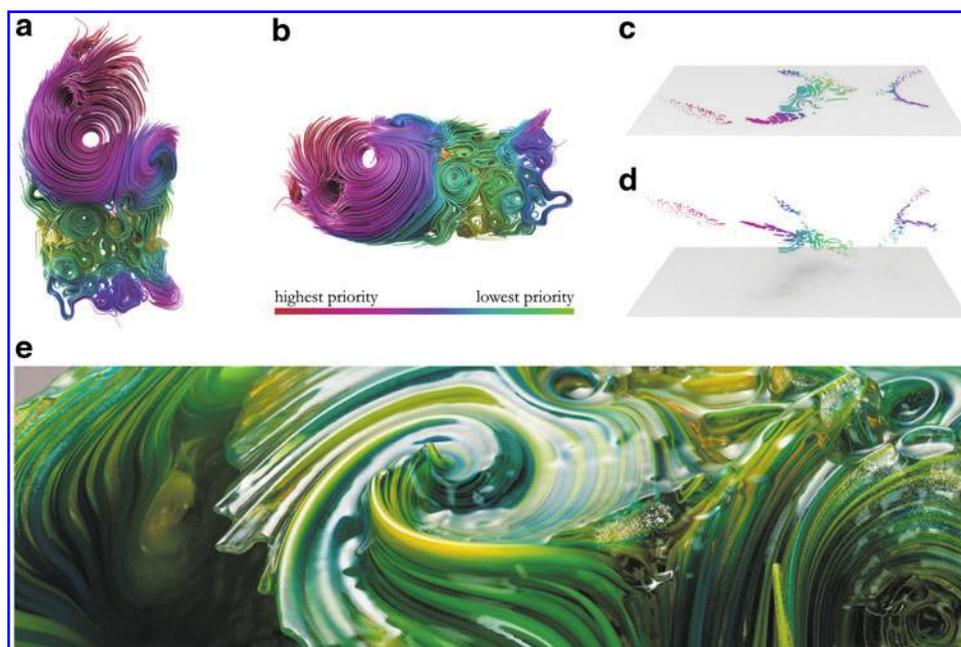
FIG. 2. An example of data-driven priority ordering for the production of large and structurally complex objects.[21] In this example, the design consists of 15,543 polygonal tubes, curled and aligned to a predefined surface contour, that are encapsulated in a 41.2 by 30.5 by 16.7 cm hull. Every tube can be assigned a uniquely different longitudinal material gradient and priority data is given by the distance from the surface contour. **(a)** A layering priority is assigned to each vertex of the polygonal tube according to its desired visibility in the final form, which varies as a function of distance from the underlying surface; **(b)** the design is aligned to the build-tray of the printer; **(c)** a slice is generated; **(d)** visualization of the priority-sorted segments of the design in the z-direction before rasterization; **(e)** resulting 3D printed model produced on an Objet 500 Connex3. Photo: Yoram Reshef, courtesy of Mediated Matter.

example, point-clouds and meshes are transferred to a volume domain, and can then be used to influence and compute heterogeneous material distributions. A typical example of external data can include a voxel grid containing an n-dimensional property per voxel, describing relative material distributions, where each voxel describes a probability for a material to be deposited. As such, the provided volume can be coarser than the actual resolution of the printer whereby an actual material droplet description will be computed from the coarser volume during slice-time. We can, therefore, separate object representation and material representation for the purpose of slicing. Figure 1(f) illustrates an example where several different material computation domains can be combined through common layering operations. Finally, Figure 1(g) shows the process of material dithering, using a modified version of Floyd and Steinberg[14] error diffusion dithering, where—for each material available to the 3D printer—a set of complementary slices is generated. An example of this is shown in Figure 3. These slices are directly input to a custom bitmap-printing system which controls the deposition of
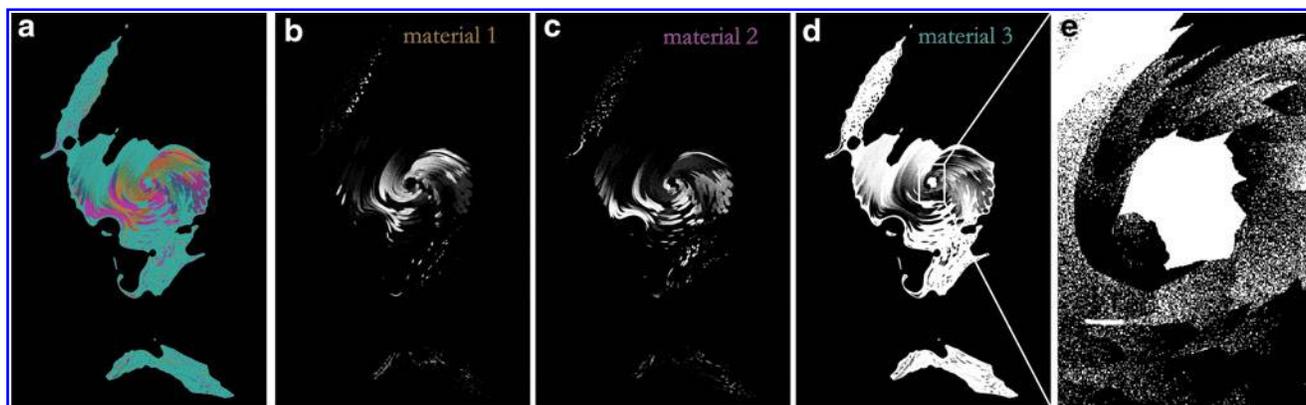

FIG. 3. Object cross-section illustrating variations in material composition of an object that is 3D printed with three different materials. **(a)** Shows the composition of all three materials. **(b–d)** Contain bitmaps that specify the droplet deposition for every material per object slice. **(d)** Shows a close-up of **(c)** whereby *white* pixels indicate material droplets deposited at each location.

FIG. 4.   A collection of three general examples of the data-driven material modeling approach, illustrating an array of internal material compositions achieved through the implementation of the described methods to achieve visually complex patterns. Such material compositions are uniquely obtained through our computational framework in combination with on-slice-time advection. The first *row* shows an example of advection driven by a given velocity field. The second *row* shows a volumetric data set where advection in the normal direction is used to create a diffusive effect in dense areas. The third *row* shows a periodic implicit function perturbed by a velocity field. For each set of 3D-printed objects, the two photographs depict the object from different viewing angles. All examples were produced on a Stratasys J750 full-color multimaterial 3D printer in collaboration with Stratasys Ltd. Photos: Mediated Matter.

material droplets by the 3D printer, such that no segmentation of material dithered slices to STL files is needed. This allows the production of objects with large volumes while still allowing for continuous material distributions.

To leverage the possibilities enabled by the design of data-driven material property variation during slice-time, we showcase function-driven advection as one example for a hybrid method to generate and influence high-resolution and heterogeneous material distributions. We denote by $m(t_0, x(t_0))$ an initial material distribution and describe the evolution of m through a velocity field $v(x)$, defined at all positions, by the advection equation $\frac{\partial m}{\partial t} + \nabla m \cdot v(x(t)) = 0$. Using the framework shown in Figure 1, we use a coarse volumetric representation of the initial material distribution of the confining object, as well as either a functionally defined or an externally given vector field, as a secondary

volume data set, in the on-slice-time data-transfer and data-modification step shown in Figure 1(f). Lagrangian paths can be generated by integrating the flow. By performing a few steps of semi-Lagrangian advection[15] using a fourth-order Runge–Kutta method, on only a few slices at a time, we can defer and distribute complex computations toward individual slice generation. Further modification can be achieved such that a simple diffusion term can be incorporated, or materials can be perturbed along the gradient of a predefined distance field. This, combined with the framework described earlier, enables the evaluation and transfer of data-sets in the material generation steps as shown in the design case study given next during slice generation. Further data-driven 3D-printed variations produced using a Stratasys J750 full-color printer and designed by implementing our method are presented in Figure 4.

Data-Driven Design

To demonstrate the DdMM approach in a design setting, we present *Lazarus*, a wearable mask designed to contain the wearer's last breath. The mask was designed as part of a collection whose design is ongoing, speculating on, and offering a new interpretation of the ancient death mask. Traditionally made of wax or plaster to represent a person's face after death, *Lazarus* serves as an ''air urn'' memento that is 3D printed, carrying a loved one's final exhale. As such, the mask offers a new form of portraiture, combining the wearer's facial features while serving as a spatial enclosure for their last breath. The mask's surface area is modeled after the face of the dying person, whereas its material composition is informed by the physical flow of air and its distribution across the surface. Unlike its traditional hand-made analog, the design of *Lazarus* is entirely data driven, digitally generated, and additively manufactured, approaching the resolution of the physical phenomenon that it is designed to capture. Data fetched to inform the distribution of airflow can be acquired from the wearer, or they can be digitally generated by a computational process incorporating the wearer's data, thereby creating a unique artifact that is perfectly customized to fit the wearer and his or her last breath.

For this speculative design, and its related (and specific) application, our design approach is illustrated in Figure 5 and can be implemented as follows. First, the data designated to drive the material distribution are either acquired or generated. In this example, only generated data are used; whereas—as stated earlier—external data sources can also be employed and used with the described method. These data are then transferred from the domain of their origin (e.g., a human face) to a target domain (e.g., a mask designed around the human face). As the data from the original domain are insufficient to compute material distributions in a volumetric domain, this step is necessary to render the provided data suitable for further computation and evaluation. The collected data sources are, subsequently, used to inform the generation of material-distributions. The material-generation step is performed during slice generation, and, as such, allows for the controllable design of material distribution at the resolution of the printer, while optimizing the use of available computational resources.

To simplify, we denote the closed parameterized surface (i.e., the face of the wearer) as $\partial\Omega$, and the target volume domain (the mask) as Ω, shown in Figure 5(d)—left and right, respectively. In this workflow, we implemented three different data sources to drive material generation. First, as shown in Figure 5(a), a heat map derived from
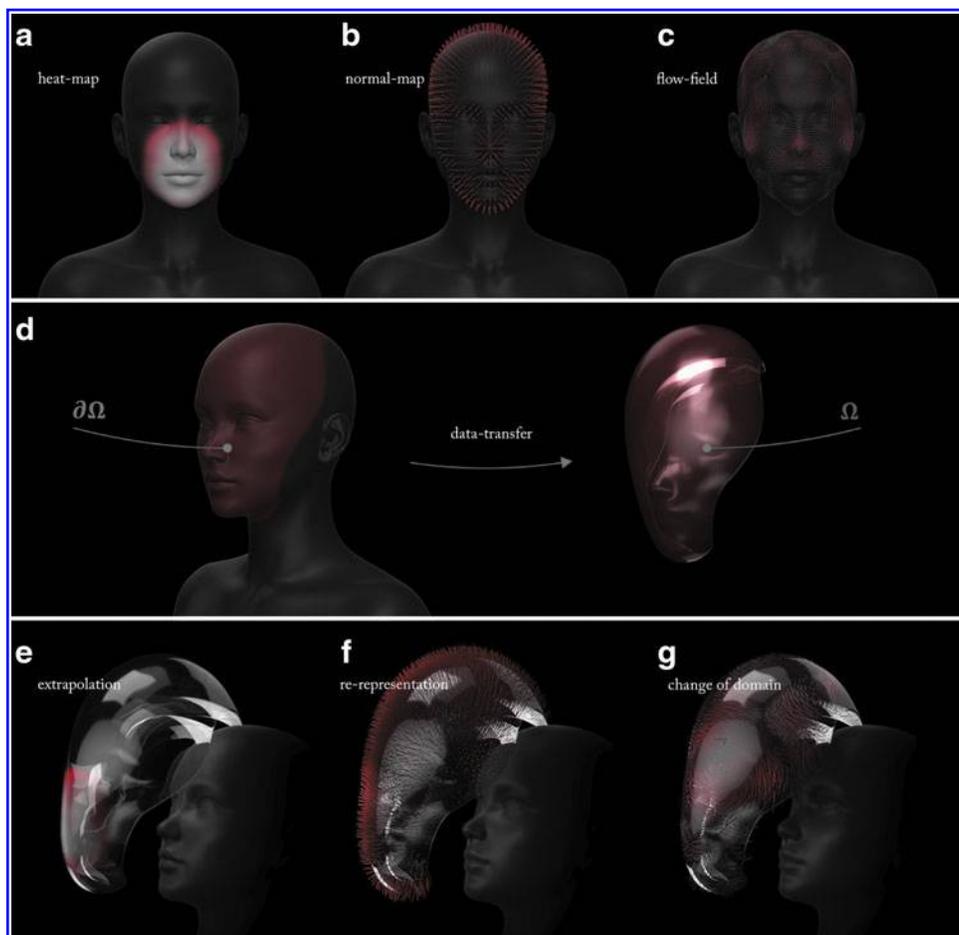

FIG. 5. Visualization of the design approach for *Lazarus*. In **(a–c)**, data sources are generated. **(a)** Shows the generated heat map; **(b)** shows the generated normal map; and **(c)** shows the velocity field computed over $\partial\Omega$. In **(d)**, the data sources are transferred to the object of interest, which is detailed in **(e–g)**.
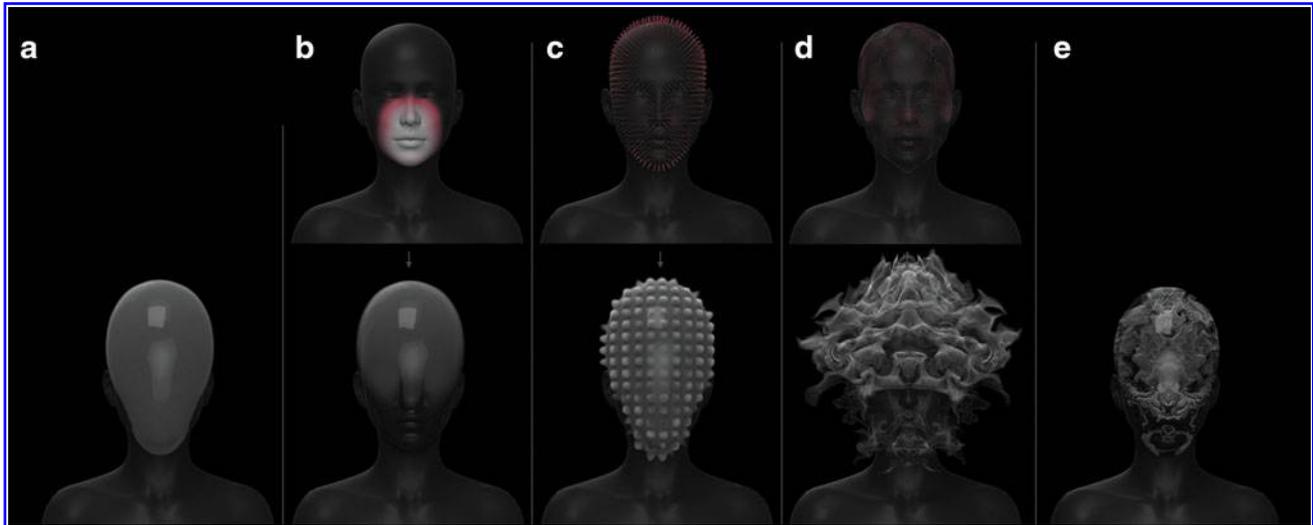
FIG. 6. Volumetric visualization of the contribution of each original data source for the generation of internal material distributions. *Gray* areas represent VeroWhite (RGD835) material, and transparent areas represent VeroClear (RGD810) material. For clarification purposes, only the distribution of the rigid *white* material in the final 3D printed prototype is emphasized (see also Fig. 7). **(a)** Initial material distribution; **(b)** contribution of the heat map as an indicator for material grading; **(c)** contribution of the normal map to align advection with the geometry of the face, here visually empathized by a displacement; **(d)** contribution of the velocity field to perturb material distribution; **(e)** final combined effects in a previsualization.
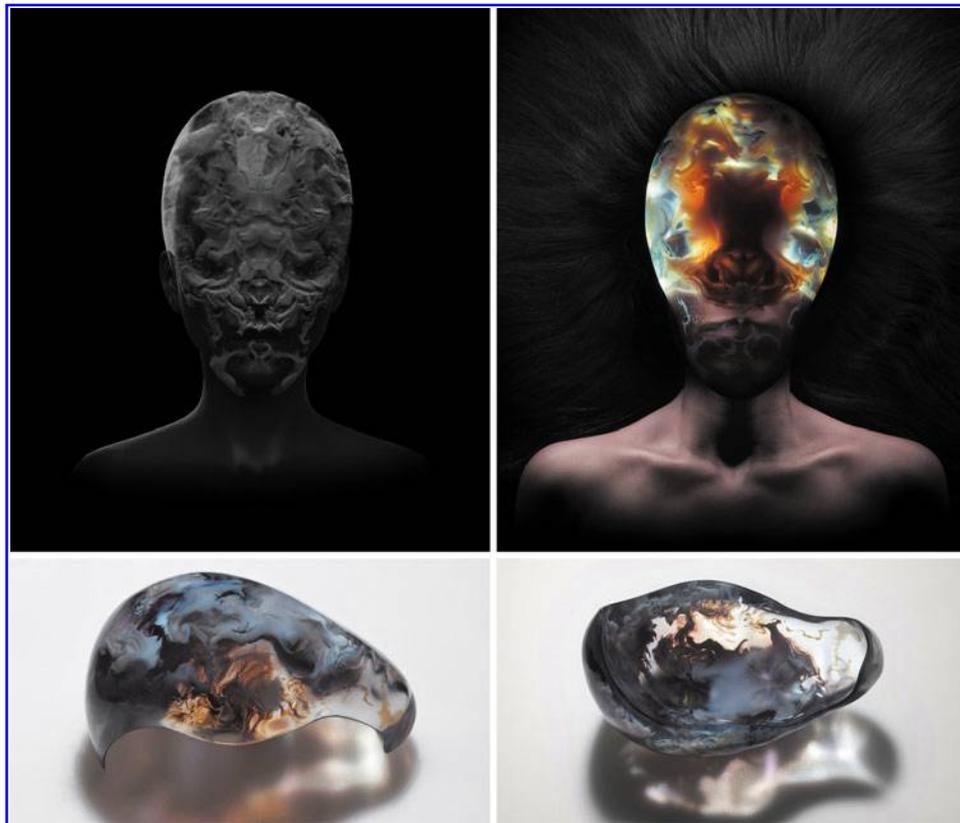

FIG. 7. *Lazarus*, 2016. Designed by Neri Oxman and the Mediated Matter Group in collaboration with Stratasys Ltd. Using a functional advection workflow, the resulting 3D printed mask—printed from rigid white and transparent materials—is shown alongside its corresponding 3D rendering. Photos: Yoram Reshef, courtesy of Mediated Matter.

solving for $u(\cdot, t) : \partial\Omega \to \mathbb{R}$ in the adapted heat equation[16] $\partial_t u(x, t) = k\Delta_\Omega u(x, t) + \frac{Q(x,t)}{c\rho}$, where Δ_Ω is the surface Laplacian, and an initial temperature $u(x, 0) = u_0(x)$ is given. Although in this case, the heat map is synthetically generated, it could equally well be acquired from a thermal imaging camera where the acquired data can be mapped to $\partial\Omega$ and similarly processed at a later time in the workflow, as described next. Second, a geometrically determined normal map as shown in Figure 5(b), from $\partial\Omega$, determined by $n(s) = \frac{(\partial_{s1}X(s) \times \partial_{s2}X(s))}{|\partial_{s1}X(s) \times \partial_{s2}X(s)|}$ is generated. Lastly, we use a velocity field [Fig. 5(c)] acquired from a computational fluid simulation mimicking simplified human respiration, where $\partial\Omega$ was used as a rigid collision object.

Figure 5(d) shows the target 3D object, which was designed specifically to fit our region of interest. On this "template," we model material distributions such that they are informed by the combined source data sets. To transfer the previously computed data sources to the volume domain, we use three different methods: extrapolation, re-representation, and a simple change of domain. First, for Ω, we generate a signed distance field[17] $d_{\partial\Omega}(x) = s_{\partial\Omega}(x) \cdot m_{\partial\Omega}(x)$, and $m_{\partial\Omega}(x) = \inf_{y \in \partial\Omega} d(x, y)$ and $s_{\partial\Omega}(x) = \{-1 \text{ if } x \text{ is interior } \partial\Omega, 1 \text{ if } x \text{ is exterior } \partial\Omega\}$,; similarly, we generate $d_\Omega = s_\Omega(x) \cdot m_\Omega(x)$, and $m_\Omega(x) = \inf_{y \in \Omega} d(x, y)$ and $s_\Omega(x) = \{-1 \text{ if } x \text{ is interior } \Omega, 1 \text{ if } x \text{ is exterior } \Omega\}$. For the heat map, we use a one-way extrapolation[18] of u from the interface along the normal direction such that $u + (\nabla u \cdot \nabla d_{\partial\Omega}) = 0$, as depicted in Figure 5(e). For the normal map, we choose to re-represent by ∇d_Ω instead of the surface normal, as ∇d_Ω is defined over all of Ω. In a similar fashion, other geometric properties such as curvature can be made useable to the volumetric domain. Finally, for the velocity field in Figure 5(g), we simply change the region where the field is sampled from $\partial\Omega$ to Ω. We note that the transfer step is not necessary if the provided data are already specified in the target domain. However, this example serves to outline how this transfer can be accomplished if the provided data sources are not specified as needed.

From these transferred data, we compute material distributions by implementing a three-step strategy. The contribution of each external data source is shown in Figure 6, where the first material is depicted as opaque, and the second is depicted as transparent. The heat map provides coarse initial guidance for the grading of material distributions, such that areas with high temperature use the first, transparent material whereas regions with low temperature use the second, opaque material. Afterwards, the velocity field perturbs material voxels according to the advection process described earlier. The normal field, in turn, aligns the flow and confines the emerging patterns to the contour of the face as well as to its surrounding boundary, by projecting the velocity to the gradient of $d_{\partial\Omega}$. As described earlier, by providing data sources during the generation of each slice, this process can be carried out per slice. This allows the material distribution to be computed at the resolution of the printer without requiring significant computational overhead, and, as such, high spatial complexity in the patterns generated can be achieved.

The resulting object was produced on a Stratasys Objet500 Connex3 printer[19] with opaque VeroWhite (RGD835) and optically transparent VeroClear (RGD810) materials, and it is shown in Figure 7. Throughout the entire design process,

the sequential design iterations were reviewed using standard volumetric visualization methods,[20] as shown in Figure 7.

The case study in this example is design driven, whereas the methods described earlier can be employed for many different applications. For example, this method can be used for direct visualization of data sets, such as z-stacks acquired from biomedical imaging studies, physical visualization of multi-field computational simulations, or visualization of point-clouds acquired from geospatial sources. Furthermore, these external data sets could be functionalized and used for the evaluation of heterogeneous material modeling methods. This could potentially allow for the production of materially optimized prosthetic sockets,[4] in finite element analysis for material optimization, or even materially adapted habitats for microbial assemblages.

Conclusion

The DdMM computational approach and its related case study presented here serve to demonstrate a DdMM workflow, combining slice processing and material distribution generation with high-resolution bitmap-based 3D printing. It provides a powerful tool for the generation of complex 3D objects with volumetric heterogeneous material distributions.

In addition to capturing, processing, generating, and digitally fabricating complex volumetric material distributions shown here, the DdMM computational approach and its related methods can contribute to a wide array of applications, including the production of high-resolution lens arrays, detailed surface topographies and lattice structures, and protocols associated with the retrieval of material properties from geometric representations. Such applications and related protocols could be produced with on-slice-time methods at the native resolution of the printer, without the need to design or generate additional geometrical content, and as such with minimal memory overhead.

Acknowledgments

Author Disclosure Statement

References

1. Oxman N. Projects. Available at http://materialecology.com/projects (accessed May 6, 2016).
2. Hansmayer M. Projects. Available at www.michael-hansmeyer.com/projects/projects.html?screenSize=1&color=1 (accessed May 6, 2016).
3. Sagi O. PolyJet Matrix™ Technology. Rehovot, Israel: Objet Geometries Ltd., 2009.
4. Doubrovski EL, Tsai EY, Dikovsky D, Geraedts JMP, Herr H, Oxman N. Voxel-based fabrication through material

property mapping: A design method for bitmap printing. Comput Aided Des 2015;60:3–13.

5. Chandru V, Swami M, Prakash EC. Voxel-based modeling for layered manufacturing. Comput Graph Appl 1995; 15:42–47.

6. Chen M, Tucker JV. Constructive volume geometry. Comput Graph Forum 2000;19:281–293.

7. Cho W, Sachs EM, Patrikalakis NM, Troxel DE. A dithering algorithm for local composition control with three-dimensional printing. Comput Aided Des 2003;35: 851–867.

8. Chiu WK, Yu KM. Direct digital manufacturing of three-dimensional functionally graded material objects. Comput Aided Des 2008;40:1080–1093.

9. Vidimče K, Wang SP, Ragan-Kelley J, Matusik W. Open-fab: A programmable pipeline for multi-material fabrication. SIGGRAPH/ACM Trans Graph 2013;32:136.

10. Kou XY, Tan ST. Heterogeneous object modeling: A review. Comput Aided Des 2007;39:284–301.

11. Biswas A, Shapiro V, Tsukanov I. Heterogeneous material modeling with distance fields. Comput Aided Geom Des 2004;21:215–242.

12. Siu YK, Sooi TT. Modeling the material grading and structures of heterogeneous objects for layered manufacturing. Comput Aided Des 2002;34:705–716.

13. Liu X, Shapiro V. Random heterogeneous materials via texture synthesis. Comput Mater Sci 2015;99:177–189.

14. Floyd RW, Steinberg L. An adaptive algorithm for spatial greyscale. Proc Soc Inf Display 1976;17:75–77.

15. Stam J. Stable fluids. In: Proceedings of the 26th Annual Conference on Computer Graphics and Interactive Tech-niques. ACM Press/Addison-Wesley Publishing Co., New York, NY, 1999; pp. 121–128.

16. Walker SW. The Shape of Things: A Practical Guide to Differential Geometry and the Shape Derivative. Philadelphia, PA: SIAM, 2015; pp. 83–84.

17. Jones MW, Bærentzen JA, Sramek M. 3D distance fields: A survey of techniques and applications. IEEE Trans Vis Comput Graph 2006;12:581–599.

18. Osher S, Fedkiw R. Level Set Methods and Dynamic Implicit Surfaces. New York: Springer Science & Buisness Media, 2006.

19. Stratasys. OBJET500 CONNEX3. Available at http://web.stratasys.com/rs/objet/images/SSYS-WP-Objet500%20Connex3.pdf (accessed May 6, 2016).

20. Levoy M. Efficient ray tracing of volume data. ACM Trans Graph 1990;9:245–261.

21. Oxman N. Wanderers—An Astrobiological Exploration. Available at http://materialecology.com/projects/details/zuhal (accessed May 6, 2016).

Address correspondence to:
Neri Oxman
Mediated Matter Group
Media Lab
Massachusetts Institute of Technology
75 Amherst Street
E14-433C
Cambridge, MA 02139

E-mail: neri@mit.edu

This article has been cited by:

1. Bader Christoph, Patrick William G., Kolb Dominik, Hays Stephanie G., Keating Steven, Sharma Sunanda, Dikovsky Daniel, Belocon Boris, Weaver James C., Silver Pamela A., Oxman Neri. 2016. Grown, Printed, and Biologically Augmented: An Additively Manufactured Microfluidic Wearable, Functionally Templated for Synthetic Microbes. *3D Printing and Additive Manufacturing* **3**:2, 79-89. [Abstract] [Full Text HTML] [Full Text PDF] [Full Text PDF with Links]